Rock fall, avalanche and debris flow sediment transport in the upper Kaunertal catchment, Ötztal Alps, Austria

Hilger, Ludwig, Tobias Heckmann, Jana Dusik, Florian Haas, Martin Näher & Michael Becht[1]
[1]Cath. Univ. Eichstaett-Ingolstadt, Physical Geography, Eichstaett, Germany (l.hilger@ku.de)

Introduction

The estimation of catchment-scale sediment transport by hillslope processes like ROCK FALL, DEBRIS FLOWS or AVALANCHES relies on the regionalisation of local measurements. Here, we show the framework for a regionalisation of the mentioned three processes by the example of a case study in the Upper Kaunertal, Austrian Central Alps (62.5 km²).

Study Area

- Kaunertal valley in the Ötztal Alps (Austrian Central Alps).; tributary of the Upper Inn river system and is drained by the Fagge brook; underlain by crystalline rocks (siliceous para- and orthogneiss); landscape dominated by glacial landforms and two main glaciers that are rapidly shrinking (Abermann et al. 2009).

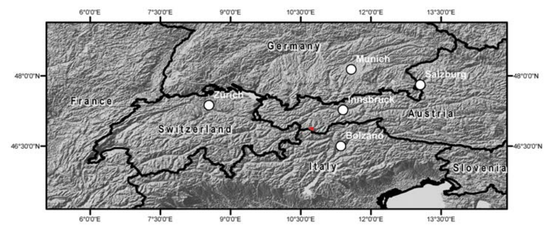

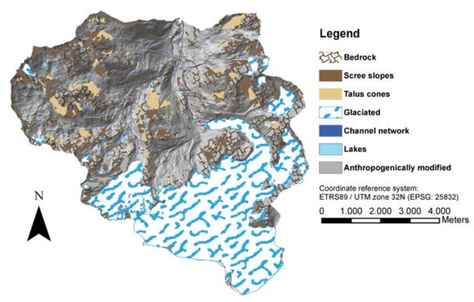

a) LiDAR survey, DEM construction & geomorphological mapping

- full-waveform ALS survey (September 2012) using Riegl LMS-Q680i (λ = 1550 nm) sensor → point density Ø 10 pts m^{-2} ; 72 fight strips adjusted and georeferenced using mountain hut roofs as tie surfaces by Philipp Gira / TU Vienna (Kager, 2004); resulting data (*780 Mio. points) now stored in spatial Postgres / PostGIS database (Rieg et al. 2013).
- only last returns used; flying points and measurement errors removed by algorithms based on point neighbourhood statistics; region growing preceded by parameter-controlled segmentation and a rule-based classfier for classification (c.f. Ying Yang and Foerstner, 2010; Bremer et al. 2013). Software package LIS (http://www.laserdata.at) used.
- geomorphological map prepared at a scale of 1:6000. Field data, literature consideration, orthorectifed aerial images of different temporal volumes and various DEM-derived land surface parameters used. Moving-window based delineation of rock wall sections.
- map conceptionalised to serve the aim of model-based connectivity analysis.Using standard symbolology set forth by Kneisel et al. (1998), does not lend itself to GIS-based analysis (areal proportion of landform types, analysis of landform topology etc). Hence, the map was also constructed with non-overlapping polygon objects representing, in most cases, sediment storage landforms, but also areas of geomorphic process activity

b) Disposition analysis using the methodology of Loye et al. (2009)

c) Measurement of rockfall rates

- nets with mesh size two mm; 60 cm high steel fences set up to prevent particles from leaving the nets downslope;
- „distance nets“, installed at two sites (c.f. Krautblatter et al., 2012); gathered rockfall particles mechanically weighted in the field
- rock densities determined in the lab (2.7 g cm^3 for gneiss & 3.1 g cm^3 for amphibolites)

d) Determination of collector net sediment contributing areas

Three different approaches for delineating SCA: i) Flow direction algorithm (see Marqunez et al., 2003), ii) expert-based mapping using aerialphotos, field experience and the DEM, and iii) back-tracing of modelled rockfall trajectories using a numerical simulation.

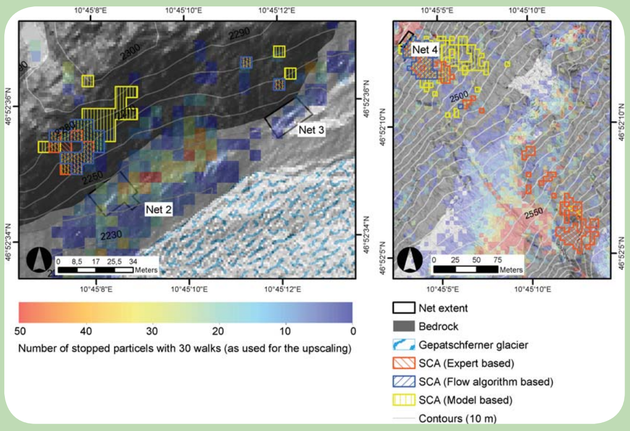

Fig.: Sediment contributing areas for nets 2, 3 and 4 according to the three dierent SCA caclulation scenarios and number of stopped particles when running the model with 30 random walks

e) Modelling and analysis of rockfall trajectories

- we apply the rockfall model described in detail by Wichmann and Becht (2005, 2006). This model has been extended, among others, with options to create edgelists (Heckmann and Schwanghart, 2013).
- calibration in carefully selected sections of the study area; qualitative model validation with rockfall event (c.f. fig. X)
- The results of the trajectory model consist of raster maps of maximum particle velocity and number of stops (c.f. fig. X), and a table (which is referred to as an edgelist). The edgelist contains, for each trajectory, the ID of each source and target raster cell, and the ID of each source and target landform (this may be the ID of each polygon of the digital geomorphological map, or an ID for the storage type, respectively).

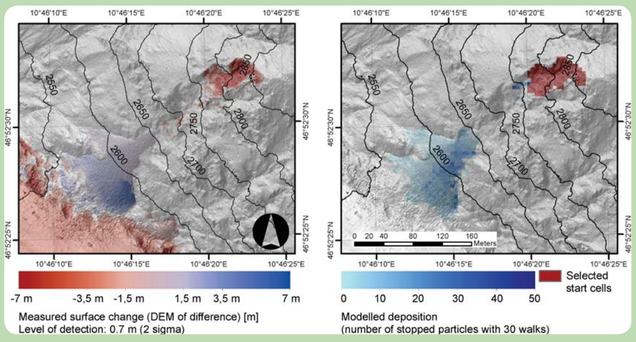

Fig.: Surface changes measured by multitemporal airborne LiDAR (left) and modelled deposition area (right). The area of negative surface change in the southwestern corner of the left map is part of the tongue of the Gepatschferner showing ablation

f) Routing of rockfall masses along the modelled trajectories

- stochastical assignment of flux rates to each modelled rockfall trajectory sampled from a PDF fitted to a data set (n=38) consisting of i) our own measurements, ii) data from literature review of studies related to recent (i.e. recently measured, and not inferred from talus volume) rates of rockfall, mostly from alpine settings.
- All mass fluxes of trajectories that have common start and target nodes are summed up. Finally, the sediment budget can be evaluated on the basis of graph nodes (rockfall initiation or deposition on original raster cells) or aggregates of the latter (polygons of the geomorphological map, or grouped by landform type).

a) Budgeting

Sediment transport by debris flows can be quantified using multi-temporal high-resolution DEMs („the so-called morphological method“). The disposition areas of 156 debris flow event were mapped on orthorectified historical aerial images and raw DTMs of difference (DoDs) representing 10 different time periods. Then, four different workflows were used to arrive at the debris flow volume, depending on the data available for the respective mapped debris flows:

a) differencing of georeferenced TLS-data
b) differencing of georeferenced ALS-data
c) differencing of ALS-data and a reconstructed pre-event surfaces
d) estimation of the volume based on a fitted relationship between planimetric debris flow disposition area and volume

Later, for each disposition area of the debris flows in categories a)-c) (#90), DEMs were constructed for each time steps using the method of moving planes which also returns grids of the standard deviation of the residuals resulting from the plane fitting for each timestep (σ_1 and σ_2). These were used to arrive at a grid of cellwise propagated error (σ_c) following the methodology described in Taylor (1997):

$$\sigma_c = (\sigma_1^2 + \sigma_2^2)^{0.5}$$

T-values for each cell were calculated to relate the raw cell difference to the propagated error:

$$t = \frac{z_1 - z_2}{\sqrt{\sigma_1^2 + \sigma_2^2}}$$

Then, probabilistic thresholding at the 95% confidence level was used to sort out DoD values considered to result from measurement errors. The error was also propagated cellwise into volumes and the significant volume measured within a debris flow deposition area was recorded for the event:

$$\sigma_v = d^2 \left(\sum_{i=1}^{I} \sum_{j=1}^{J} [\sigma_{1ij}^2 + \sigma_{2ij}^2] \right)^{0.5}$$

, where d is the cellsize and i, and j iterators for cell rows and columns in the error grids and σ_v is the propagated error in volume

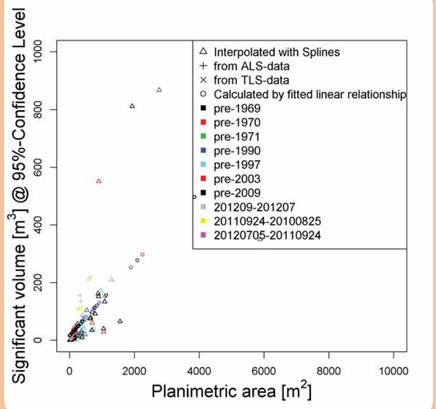

Fig.: Area-Volume scatterplot for 153 debris flow events in the study area (1953-2012)

b) First exploratory magnitude-frequency analysis

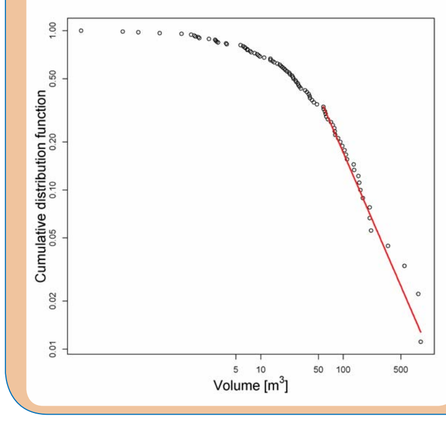

Fig.: Cumulative empiral distributions of the 153 debris flow volumes with power law and log-normal distribution fits

It has often been reported that the distribution of volumes of gravitational mass movements follow a simple power law of the form:

$p(x) = ax^{-\alpha}$ (e.g. Bennett et al., 2012,)

We fitted this and, as a comparison, a log-normal distribution to our data using the maximum liklihood method of (c.f. Clauset et al., 2009). Right now, the log-normal distribution looks more promising, but further work on the subject will be undertaken.

Sediment transport by avalanches was determined by mapping full-depth avalanche deposits in the field in early 2013 and 2014. Heterogenous sediment cover was classified into five classes (Sks, see below). The spatial distribution of these classes was mapped for each full-depth avalanche and debris on multiple test plots of each sediment class were collected from different avalanches. The sediment from the test plots was quantified in the laboratory and mean sediment masses for each sediment class were combined with the mapping results to arrive at estimates for the whole catchment.

Our investigations from winter 2012/2013 resulted in a erosion rate of c. 8.75 t/km².

Fig.: Mapped sediment coverage classes for an avalanche in the Fernergries area (right) and representative test plots for the different classes (below))

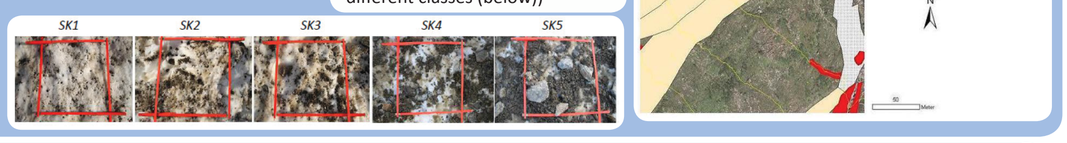

g) Results

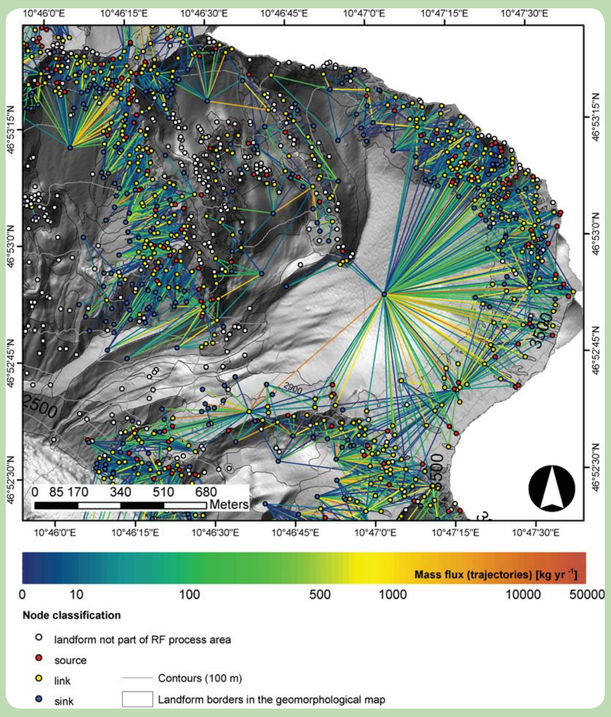

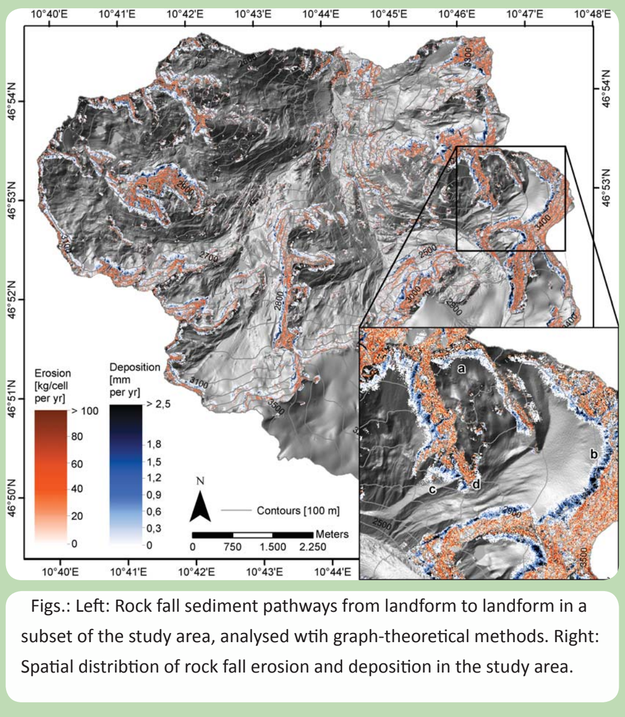

Figs.: Left: Rock fall sediment pathways from landform to landform in a subset of the study area, analysed wtih graph-theoretical methods. Right: Spatial distribtion of rock fall erosion and deposition in the study area.

Acknowledgements:

- We would like to thank Philipp Glira from the TU Vienna for his work in adjusting and georeferencing the airborne LiDAR data and repated valuable advice concerning 3D point data handling.
- Thanks also to all students assisting in the field and in referencing the TLS data: Florian Riehl, Philipp Rumohr, Kerstin Schlobies and Sebastian Wiggenhauser

References:

ABERMANN, J.; LAMBRECHT, A.; FISCHER, A.; KUHN, M. (2009): Quantifying changes and trends in glacier area and volume in the Austrian Ötztal Alps (1969-1997-2006). In: The Cryosphere 3 (2), S. 205–215.
BENNETT, G. L.; MOLNAR, P.; EISENBEISS, H.; MCARDELL, B. W. (2012): Erosional power in the Swiss Alps: characterization of slope failure in the Illgraben. In: Earth Surf. Process. Landf. 37 (15), S. 1627–1640. Online verfügbar unter http://dx.doi.org/10.1002/esp.3263.
CLAUSET, A.; SHALIZI, C. R.; NEWMAN, M. E. J. (2009): Power-law distributions in empirical data. In: SIAM review 51 (4), S. 661–703.
HECKMANN, T.; HILGER, L.,; VEHLING, L.; BECHT,, M. (2O14): Integrating eld measurements, a geomorphological map and stochastic modelling to estimate the spatially distributed rockfall sediment budget of the Upper Kaunertal, Austrian Central Alps. Geomorphology (in review).
KAGER, H. (2004): Discrepancies between overlapping laser scanner strips - simutaneous fitting of aerial laser scanner strips. In: International Archives of Photogrammetry, Remote Sensing and Spatial Information Sciences. British Hydrological Society International Conference. London, July 12-16, 2004 (1), S. 555–560.
LANE, S. N.; WESTAWAY, R. M.; MURRAY H., D. (2003): Estimation of erosion and deposition volumes in a large, gravel-bed, braided river using synoptic remote sensing. In: Earth Surf. Process. Landf. 28 (3), S. 249–271, zuletzt geprüft am 10.01.2013.
TAYLOR, J. R. (1997): An introduction to error analysis. The study of uncertainties in physical measurements. Sausalito, Calif: Univ. Science Books.